

Indole-Based NLOphoric Donor- π -Acceptor Styryl Dyes: Synthesis, Spectral Properties and Computational Studies

Santosh Chemate¹ · Nagaiyan Sekar¹

Received: 31 January 2016 / Accepted: 4 August 2016
© Springer Science+Business Media New York 2016

Abstract Donor- π - acceptor styryl chromophores based on indole core were synthesized by Knoevenagel condensation of N-ethyl indole-3-carbaldehyde and different active methylene compounds. The absorption and emission properties of these dyes in different solvents were studied. The dyes displayed a broad absorption maximum in the UV and visible region between 397 and 469 nm with FWHM, 50 to 75 nm. Due to the extended π – conjugated systems this styryl chromophores shows strong intramolecular charge transfer characteristics. The dyes showed solid state emission and emission in solid state was red shifted as compared to their emission in less polar solvents. Density Functional Theory [B3LYP/6–311 + G(d)] computations were used to correlate the structural, molecular, electronic and photo physical parameters of styryl dye with experimental study. Synthesized dyes were confirmed by using FT-IR, ¹H NMR, ¹³C NMR and HRMS spectral analysis.

Keywords Indole-3-carbaldehyde · Styryl · Solid state fluorescence · DFT

Introduction

During the past few decades, the donor- π -acceptor (D- π -A) chromophores have attracted considerable interest due to their

Electronic supplementary material The online version of this article (doi:10.1007/s10895-016-1901-5) contains supplementary material, which is available to authorized users.

✉ Nagaiyan Sekar
n.sekar@ictmumbai.edu.in

¹ Department of Dyestuff Technology, Institute of Chemical Technology, Mumbai 400 019, India

potential applications in electro/photoactive materials, such as dye sensitized solar cells [1, 2] laser dyes [3], nonlinear optical (NLO) materials [4, 5], organic light-emitting diodes (OLEDs) [4] and organic field-effect transistors (OFETs). Owing to their excellent photophysical properties. D- π -A chromophores are widely used in sensitizers [6, 7], photographic materials [8], optical recording materials [9–11], photo initiators for free radical polymerization [12] and fluorescent probes [13]. The styryl chromophores derived from indole heterocycle constitute a part of various dye materials [14–19] and have been used for dyeing of keratin fibers [20], lightning keratin materials [21] and dyeing of synthetic fibres. Organic fluorophores exhibiting solid state fluorescence efficiency have received increasing attention owing to their potential application in OLEDs [22–24], organic field-effect transistors [25], in the field of lasers [26], photovoltaic cells [27], sensors for biological molecule [10, 28–31] and bio-cell imaging [32].

The donor- π -acceptor styryl chromophore shows strong intramolecular charge-transfer (ICT) characteristics because the donor group (D) is an electron-rich unit, linked through a π bridge spacer to the electron-acceptor group (A). It is easy to modify their physical and chemical characteristics by tuning different donor or acceptor units. In D- π -A molecules the electron-rich nitrogen or sulphur atom usually acts as electron donor. The absorption and emission of the molecules are solvent dependent and the styryl derivatives show aggregation induced emission [32, 33]. The emission of organic dyes is effectively suppressed in solid state due to aggregation in planar - π - conjugated system based on π - π interaction or the formation of excimers [34–36]. There has been considerable interest in preparing indole based donor- π -acceptor styryl dyes which retain their photophysical properties in the solid state [37, 38]. The absorption and emission mainly depend on conjugation, planarity and rigidity in the molecule as well as

on solvent polarity. It is our endeavor to look into extensively conjugated fluorescent dyes in this chromophoric system. The indole based D- π -A styryl chromophore reported in this paper shows excellent solid state emission between 487 nm to 551 nm. DFT study has been carried out using B3LYP/6-311 + G(d) to understand photophysical properties of synthesized molecules.

Experimental Section

Materials and Equipments

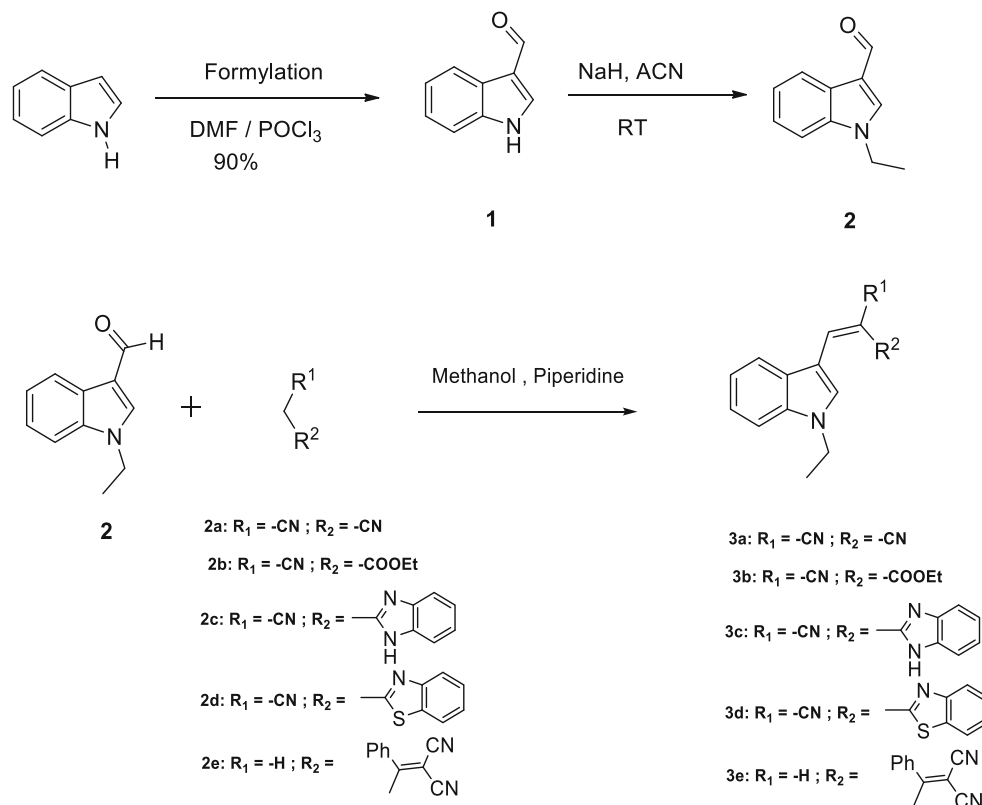
All the reagents and solvents were purchased from S. D. Fine Chemicals Ltd. and they were used without further purification and all the solvents were used of spectroscopic grade. The absorption spectra of these dyes were recorded on Perkin Elmer UV-visible spectrophotometer, and emission spectra were recorded on Varian Cary Eclipse fluorescence spectrophotometer (Varian, Australia) using 1 cm length quartz cells. The emission spectra was recorded by exciting the molecules at their maximum wavelength of absorption in the respective solvents. The melting points were recorded on instrument from Sunder Industrial Product Mumbai by using open capillary and are uncorrected. The FT-IR spectra were recorded on a Jasco 4100 Fourier Transform IR instrument (ATR accessories). ¹H NMR spectra were recorded on a Varian 500 MHz

USA instrument using TMS as an internal standard. Mass spectra were recorded on Finnigan Mass spectrometer. The chemical shift values are expressed in δ ppm using DMSO-*d*₆ as a solvent and TMS as an internal standard. DFT calculations were performed on a HP workstation XW 8600 with Xeon processor, 4 GB RAM and Windows Vista as operating system. The software package used was Gaussian 09 W [39]. The ground state geometry was optimized at B3LYP level of theory and 6-311 + G (d) as a basis set (Scheme 1).

Computational Methods

Gaussian 09 program package was used for geometry optimization of synthesized styryl dyes [39]. Geometry optimization of molecules in their ground state was carried out in both vacuum and solvent by using polarizable continuum model (PCM) [40]. Ground state (S_0) geometry of the dyes in gas and solvent was optimized in their C₁ symmetry using DFT [41]. The Becke's three parameter exchange functional (B3) [42] combining with nonlocal correlation functional by Lee, Yang and Parr (LYP) [43] and basis set 6-311 + G(d) was used for all the atoms. Same method was used for vibrational analysis to verify that the optimized structures correspond to local minima on the energy surface. Time Dependent Density Functional Theory (TDDFT) computations were used to obtain the vertical excitation energies and oscillator strengths at

Scheme 1 Synthesis of 3a-e



the optimized ground state equilibrium geometries at the same hybrid functional and basis set [41].

Relative Quantum Yield Calculations

The quantum yields of compounds **3a** to **3e** in different solvents were evaluated. The fluorescence quantum yields (Φ_f) at room temperature were measured relative to quinine sulfate in 0.1 N H₂SO₄ ($\Phi_f = 0.51$) [44]. The absorption and emission characteristics of the standards and the compounds in polar as well as non-polar solvents were measured at different concentrations. The emission intensity values were plotted against absorbance values and linear plots were obtained. Gradients were calculated for the compounds in each solvent and for the standards. All the measurements were done by keeping the parameters such as solvent and slit width constant. The relative quantum yields of synthesized compounds in different solvents were calculated by using Eq. (1). The refractive indices of the solvents have been taken from literature [45].

$$\Phi_x = \Phi_{st} \times \frac{\text{Grad}_x}{\text{Grad}_{st}} \times \frac{\eta_x^2}{\eta_{st}^2} \quad (1)$$

Where:

Φ_x = Quantum yield of compound.

Φ_{st} = Quantum yield of standard sample

Grad_x = Gradient of compound.

Grad_{st} = Gradient of standard sample.

η_x = Refractive index of solvent used for synthesized compound.

η_{st} = Refractive index of solvent used for standard sample.

Experimental Details

Synthesis of Compound 1

Phosphorous oxychloride (POCl₃) (7.65 g, 0.05 mol) was added drop wise to N, N-dimethyl formamide (15.4 ml, 0.20 mol) at 5–10 °C with constant stirring under nitrogen atmosphere. The complex formed was stirred for 30 min. The solution of indole (5.3 g, 0.0453 mol) in DMF (20 ml) was slowly added to complex and stirred at 35 °C for 1 h, ice was added, followed by 20 % aq. sodium hydroxide (NaOH), and the mixture was refluxed for 6 h. The reaction mixture was cooled to room temperature and then poured into cold ice water, and the precipitated product was collected, washed with water and dried. Yield: 95 %, Light yellow solid, m.p. 190–192 °C (190–192 °C) [46].

Synthesis of Compound 2

Indole-3-carbaldehyde (1.45 g, 0.01 mol) dissolved in dry acetonitrile (30 ml) and cooled to 0 °C and NaH (60 % in

oil) (0.44 g, 0.011 mol) was added and stirred for 10 min under N₂ atmosphere. Then ethyl bromide (1.2 g, 0.011 mol) was added dropwise and stirred at room temperature for 2 h. The reaction mixture was filtered to remove salt formed and filtrate was concentrated to get solid product. The product was recrystallized from 95 % ethanol to get pure product. Yield: 95 %, Light yellow solid, m.p. 62 °C (60–65 °C) [47].

General Procedure for Synthesis of Compounds 3a-3e

N-Ethyl indole-3-aldehyde (1.0 mmol) was dissolved in 10 ml of dry methanol and active methylene compound (1.0 mmol) were added at room temperature. Then piperidine (0.1 mmol) was added as a catalyst and the reaction mixture was refluxed for 5 h. The progress of the reaction was monitored on TLC. The reaction mixture was filtered and solid obtained was dried. The crude products were recrystallised form aq. ethanol.

Structural Confirmations

((1-Ethyl-1H-Indol-3-Yl)Methylene)Malononitrile (3a)

Yield: 95 %, Melting Point: 148 °C, ¹H NMR (DMSO-*d*₆, 500 MHz) δ ppm: 1.41 (t, 3H), 4.41 (q, 2H), 7.33 (dd, $J = 8$ Hz & 16 Hz, 1H), 7.36 (dd, $J = 8$ Hz & 16 Hz, 1H), 7.68 (d, $J = 8$ Hz, 1H), 8.06 (d, $J = 13$ Hz, 1H), 8.54 (s, 1H), 8.65 (s, 1H), ¹³C NMR (DMSO-*d*₆, 125 MHz) δ ppm: 152.2, 136.3, 135.2, 127.9, 124.5, 123.4, 119.8, 116.4, 116.3, 112.0, 110.6, 69.5, 43.5, 15.4, FT-IR (cm⁻¹): 2213 (–CN), 1585 (–C = C-, olefinic), 1566, 1512 (–C = C-, aromatic) HRMS (EI): calcd for C₁₄H₁₂N₃, 222.1031 [M + H]⁺; found: 222.1024.

(Z)-Ethyl 2-Cyano-3-(1-Ethyl-1H-Indol-3-Yl)Acrylate (3b)

Yield: 96 %, Melting Point: 98 °C, ¹H NMR (DMSO-*d*₆, 500 MHz) δ ppm: 1.42 (t, 3H), 3.30 (s, 3H), 3.81 (s, 2H), 4.39 (q, 2H), 7.97 (d, $J = 7.0$ Hz, 1H), 7.29 (dd, $J = 7.0$ Hz & 13 Hz, 1H), 7.67 (d, $J = 8$ Hz, 1H), 7.35 (dd, $J = 7.9$ Hz & 13 Hz, 1H), 8.51 (s, 1H), 8.58 (s, 1H), ¹³C NMR (DMSO-*d*₆, 125 MHz) δ ppm: 164.3, 146.5, 136.4, 134.8, 128.1, 124.2, 123.0, 119.4, 118.4, 111.9, 109.6, 92.2, 79.6, 53.1, 42.3, 15.4, FT-IR (cm⁻¹): 2212 (CN), 1709 (carbonyl), 1617, 1589 (–C = C-, olefinic), 1589, 1516 (–C = C-, aromatic) HRMS (EI): calcd for C₁₆H₁₆N₂O₂, 269.1290 [M + H]⁺; found: 269.1284.

(Z)-2-(1H-Benzo[d]Imidazol-2-Yl)-3-(1-Ethyl-1H-Indol-3yl)Acrylonitrile (3c)

Yield: 94 %, Melting Point: 230 °C, ¹H NMR (DMSO-*d*₆, 500 MHz) δ ppm: 1.43 (t, 3H), 4.39 (q, 2H), 7.2–7.3 (m, 4H), 7.51 (d, 1H), 7.64 (dd, $J = 1.5$ Hz, 7.0 Hz, 2H), 7.99 (dd, $J = 1.5$ Hz, 7.0 Hz, 1H), 8.50 (s, 1H), 8.58 (s, 1H), 12.8 (s, 1H), ¹³C NMR (DMSO-*d*₆, 125 MHz) δ ppm: 149.3, 144.0, 137.2, 136.0, 131.1, 128.3, 123.7, 123.3, 122.0, 119.0, 118.7, 111.6, 110.1, 94.5, 79.6, 42.0, 15.6, FT-

Table 1 The UV-Vis absorption and fluorescence emission of compounds **3a-3e** in solvents of varying polarities

Entry	Solvent	λ_{abs} nm	λ_{ems} nm	Stokes Shift cm^{-1}	ϵ (Mole $^{-1}$ cm^{-1})	FWHM (nm)	f	$\sigma(1 \times 10^{-14})$	Φ
3a	DMSO	398	443	2552	25,772	54	0.4156	0.9857	0.0184
	DMF	398	442	2501	24,905	52	0.3891	0.9526	0.0242
	ACN	394	444	2858	34,227	52	0.5319	1.0295	0.0163
	MeOH	395	444	2793	26,917	52	0.4249	1.3091	0.0071
	Acetone	398	435	2137	26,145	52	0.4116	1.0000	0.0041
	DCM	397	436	2253	29,776	52	0.4554	1.1389	0.0142
	CHCl ₃	400	436	2064	38,734	50	0.6073	1.4815	0.0128
	EA	390	442	3016	27,796	52	0.4419	1.0632	0.0128
	THF	391	440	2848	27,695	52	0.4257	1.0593	0.0201
	1,4 dioxane	388	534	6849	27,177	51	0.4287	1.0394	0.0184
3b	Toluene	398	534	7047	23,986	50	0.3666	0.9175	0.0313
	DMSO	393	444	2923	25,718	54	0.4144	0.9837	0.0174
	DMF	389	441	3031	25,191	55	0.4149	0.9636	0.0205
	ACN	387	439	3060	31,187	51	0.4853	1.0072	0.0183
	MeOH	391	443	3002	26,334	53	0.4217	1.1929	0.0093
	Acetone	387	433	2745	25,712	53	0.4076	0.9835	0.0057
	DCM	392	436	2574	34,484	51	0.5317	1.3190	0.0191
	CHCl ₃	393	437	2562	35,140	53	0.5626	1.3441	0.0149
	EA	386	434	2865	27,326	51	0.4197	1.0452	0.0186
	THF	384	432	2893	27,329	51	0.4242	1.0533	0.0174
3c	1,4 dioxane	384	535	7350	26,216	51	0.4109	1.0028	0.0164
	Toluene	387	437	2957	26,966	53	0.4301	1.0314	0.0304
	DMSO	408	463	2911	37,166	66	0.6344	1.4216	0.0191
	DMF	406	461	2938	35,002	66	0.6123	1.3388	0.0211
	ACN	401	457	3055	29,688	68	0.5182	1.3312	0.0179
	MeOH	407	464	3018	34,804	64	0.6138	1.1355	0.0074
	Acetone	402	459	3089	40,285	99	0.7077	1.5409	0.0064
	DCM	412	469	2950	29,826	69	0.4996	1.1389	0.0171
	CHCl ₃	417	480	3147	28,046	71	0.4541	1.0728	0.0142
	EA	402	460	3136	44,055	66	0.7845	1.6851	0.0179
3d	THF	402	459	3089	40,057	65	0.7031	1.5322	0.0193
	1,4 dioxane	402	462	3230	41,338	66	0.53258	1.5811	0.0184
	Toluene	422	467	2283	36,142	67	0.5326	1.3824	0.0231
	DMSO	427	493	3035	32,411	69	0.4425	1.2397	0.0194
	DMF	423	485	3022	34,634	68	0.5046	1.3247	0.0231
	ACN	418	483	3219	50,269	68	0.7772	1.3710	0.0167
	MeOH	422	486	3120	35,844	67	0.5193	1.9227	0.0059
	Acetone	419	481	3076	40,192	68	0.6331	1.5373	0.0077
	DCM	420	492	3484	52,549	66	0.7629	2.0100	0.0171
	CHCl ₃	421	491	3386	54,212	68	0.7891	2.0736	0.0182
3e	EA	416	478	3118	38,738	66	0.5916	1.4817	0.0165
	THF	420	482	3063	36,611	67	0.5416	1.4004	0.0192
	1,4 dioxane	416	481	3248	331,515	67	0.5046	1.2680	0.0194
	Toluene	422	483	2993	36,311	67	0.5298	1.3889	0.0315
	DMSO	469	540	2803	20,589	72	0.3166	0.7875	0.0171

Table 1 (continued)

Entry	Solvent	λ_{abs} nm	λ_{ems} nm	Stokes Shift cm^{-1}	ϵ ($\text{Mole}^{-1} \text{cm}^{-1}$)	FWHM (nm)	f	$\sigma(1 \times 10^{-14})$	Φ
	DMF	463	535	2906	20,402	71	0.3146	0.7804	0.0214
	ACN	453	528	3136	43,562	70	0.6909	1.6313	0.0196
	MeOH	454	531	3194	42,646	71	0.6657	1.6665	0.0060
	Acetone	452	524	3039	41,909	69	0.6509	1.6030	0.0068
	DCM	455	533	3216	49,894	68	0.7602	1.9084	0.0691
	CHCl_3	457	526	2870	67,631	67	1.0259	2.5869	0.0152
	EA	447	518	3066	42,682	67	0.6521	1.6326	0.0174
	THF	452	525	3076	37,446	67	0.5673	1.4323	0.0195
	1,4 dioxane	445	514	3017	40,056	69	0.6289	1.5321	0.0179
	Toluene	453	517	3233	39,977	68	0.6215	1.5291	0.0279

FWHM Full width at half maximum, σ = Absorption cross-section, ϵ = molar extinction coefficient, f = Oscillator strength, Φ = Quantum yield

Where, MeOH Methanol, EtOH Ethanol, EA Ethyl Acetate, DMF Dimethyl formamide, DMSO Dimethyl sulfoxide, DCM Dichloromethane, CHCl_3 Chloroform, THF Tetrahydrofuran

IR (cm^{-1}): 2213 (–CN), 1637, 1620 (–C = C–, olefinic), 1592, 1531 (–C = C–, aromatic) **HRMS** (EI): calcd for $\text{C}_{20}\text{H}_{17}\text{N}_4$, 313.1453 $[\text{M} + \text{H}]^+$, found: 313.1442.

(Z)-2-(Benzo[d]Thiazol-2-Yl)-3-(1-Ethyl-1H-Indol-3-Yl)Acrylonitrile (3d) Yield: 95 %, Melting Point: 169 °C, **^1H NMR** (DMSO-*d*₆, 500 MHz) δ ppm: 1.44 (t, 3H), 4.40 (q, 2H), 7.28–7.36 (m, 2H), 7.43 (dd, $J = 8.5$ Hz, 16.5 Hz, 1H), 7.54 (dd, $J = 7.0$, 15.5 Hz, 1H), 7.67 (d, $J = 8.5$ Hz, 1H), 8.01 (d, $J = 8.0$ Hz, 1H), 8.07 (dd, $J = 8$ Hz & 17 Hz, 1H), 8.12 (dd, $J = 8$ Hz & 17 Hz, 1H), 8.49 (s, 1H), 8.57 (s, 1H), **^{13}C NMR** (DMSO-*d*₆, 125 MHz) δ ppm: 164.5, 153.6, 139.8, 136.3, 134.4, 133.2, 128.0, 127.3, 125.8, 124.0, 122.8, 122.6, 122.5, 119.6, 111.7, 110.2, 97.0, 79.6, 42.1, 15.5. **FT-IR** (cm^{-1}): 2985 (aromatic, –CH), (–CN), 1620 (–C = C–, olefinic), 1580, 1517 (–C = C–, aromatic) **HRMS** (EI): calcd for $\text{C}_{20}\text{H}_{16}\text{N}_3\text{S}$, 330.1065 $[\text{M} + \text{H}]^+$, found: 330.1058.

(Z)-2-(3-(1-Ethyl-1H-Indol-3-Yl)-1-Phenylallylidene)Malononitrile (3e) Yield: 91 %, Melting Point: 203 °C, **^1H NMR** (DMSO-*d*₆, 500 MHz) δ ppm: 1.37 (t, 3H), 4.23 (q, 2H), 7.14 (d, $J = 15$, 1H), 7.34 (m, 2H), 7.45 (d, $J = 15.5$ Hz, 1H), 7.47–7.48 (m, 2H, Ar-H), 7.59 (dd,

$J = 9.0$ Hz & 3.0 Hz, 1H, Ar-H), 7.66 (dd, 7.0 Hz & 2.0 Hz, 1H), 7.80 (dd, $J = 7.0$ Hz & 2.0 Hz, 1H, Ar-H), 8.21 (s, 1H), **^{13}C NMR** (DMSO-*d*₆, 125 MHz) δ ppm: 172.5, 144.6, 138.8, 138.1, 133.9, 131.1, 129.4, 129.3, 125.5, 124.1, 123.1, 120.4, 118.1, 115.0, 113.5, 112.2, 79.6, 41.7, 15.3, **FT-IR** (cm^{-1}): 2215 (–CN), 1592, 1504 (–C = C–, olefinic), **HRMS** (EI): calcd for $\text{C}_{22}\text{H}_{18}\text{N}_3$, 324.1501 $[\text{M} + \text{H}]^+$, found: 324.1498.

Result and Discussion

Photophysical Study

The UV-visible absorption emission spectra of the compounds **3a–3e** were evaluated in polar as well as in less polar solvents (Table 1). The styryl derivatives of indole showed red and blue shifted absorption and emission depending upon the solvent polarities. These 3-vinylindole derivatives showed more red shifted emission in polar solvents than in less polar solvents. The compound **3a** exhibited red shifted emission in polar solvents (methanol, ethanol, DMSO and acetonitrile) and blue shifted emission in less polar solvents (1, 4 dioxane, THF and

Fig. 1 Absorption and emission spectra of compound **3a** in different solvents

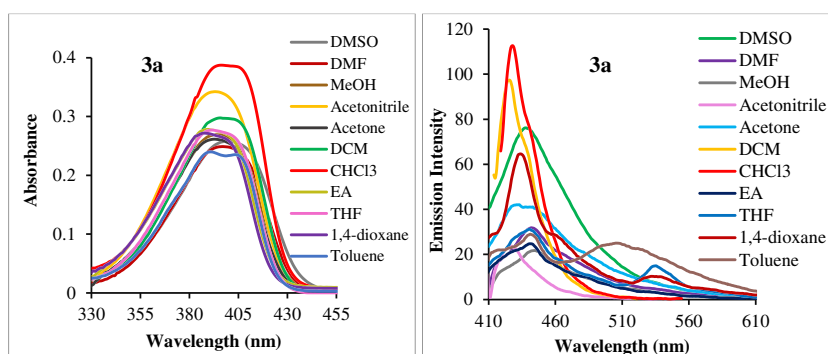
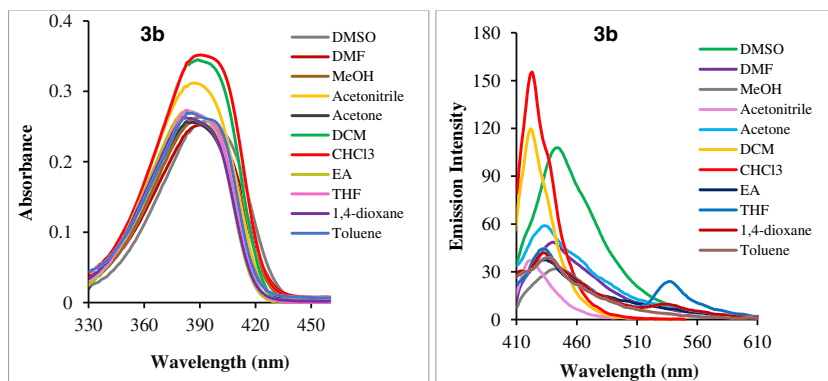


Fig. 2 Absorption and emission spectra of compound **3b** in different solvents



ethyl acetate) (Fig. 1). The similar trend was observed for the dyes **3b**, **3c** and **3d** (Figs. 2, 3 and 4). A more red shifted in absorption and emission was observed in case of compound **3e** due to extended conjugation and intramolecular charge transfer from the donor to the acceptor moiety (Fig. 5). The red shifted absorption and emission was observed for **3e** with increasing solvent polarity. All the dyes showed large Stokes shift in all the solvents. The fluorescence quantum yields of the synthesized 3-vinylindole derivatives were determined in different solvents and are tabulated in Table 1. The result showed that the fluorescence quantum yield is dependent on the solvent polarity. The compounds **3a-3c** showed two emissions peaks in nonpolar solvent like 1, 4-dioxane, toluene and THF. The quantum yield values for **3a-3e** increases with an increase in solvent polarity, but for **3a** and **3b** in toluene it showed high quantum yield ($\Phi_f = \sim 0.03$) due to twisted intramolecular charge transfer (TICT) process. As compared with the fluorescence spectra in solution, the dyes **3a**, **3b** and **3d** showed slightly red shifted solid state fluorescence emission revealing intramolecular π - π interactions present in the D- π -A molecules. The dyes **3a**, **3b** and **3e** showed more FWHM in polar solvents than in less polar solvent while no correlation in FWHM with respect to solvent polarity was observed for the dyes **3c** and **3d** (Table 1). The molar absorption cross section (σ) were determined in all the solvents and found higher in

chlorinated solvent for the dyes **3a**, **3b**, **3d** and **3e**. In the case of dye **3c** it is higher in ethyl acetate, THF and 1,4 dioxane. The values for the σ falls in the range of 0.7804 – $2.5869 \times 10^{-14} \text{ cm}^2$. The molar extinction co-efficient at λ_{max} is the highest in chlorinated solvents for the dyes **3a**, **3b**, **3d** and **3e**. In the case of dye **3c** it is higher in less polar solvents such as ethyl acetate, THF and 1,4 dioxane (Table 1). The molar extinction coefficient of the dyes varied from $24,905$ to $67,631 \text{ mol}^{-1} \text{ cm}^{-1}$.

Solid State Emission

The dyes **3a**, **3b** and **3d** showed solid state fluorescence maxima at 487, 486, and 561 nm respectively (Fig. 6). The molecule with effective intramolecular π - π interactions shows strong solid state emission intensity so that dye **3b** shows three times more intensity than the dye **3a**. The introduction of bulky substituent at the periphery of the π -conjugation system, decreases its solid state emission efficiency because it inhibits aggregation. Thus the dye **3c** and **3e** shows poor solid state fluorescence efficiency. The dyes **3c** and **3d** have benzimidazole and benzothiazole unit in acceptor part but only the dye **3d** shows a weak solid state fluorescence, and this is because in case of the dye **3d** effective charge transfer is possible because of vacant d-orbital of sulphur and such a charge transfer is not possible for the dye **3c** (Table 2).

Fig. 3 Absorption and emission spectra of compound **3c** in different solvent

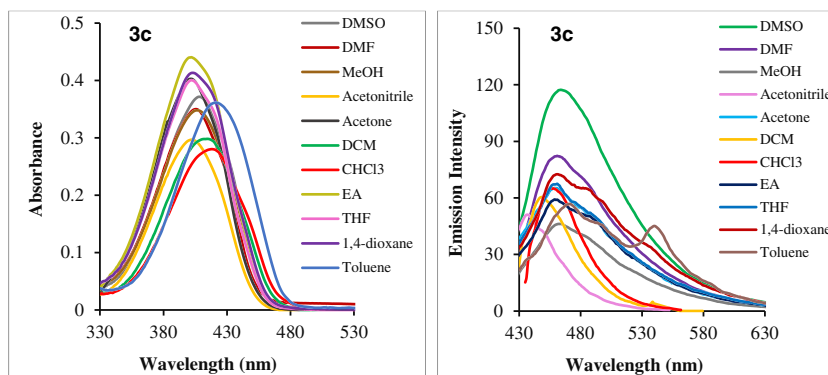
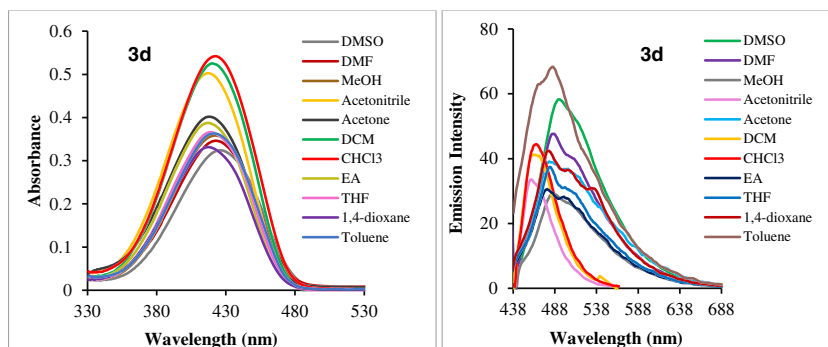


Fig. 4 Absorption and emission spectra of compound **3d** in different solvents

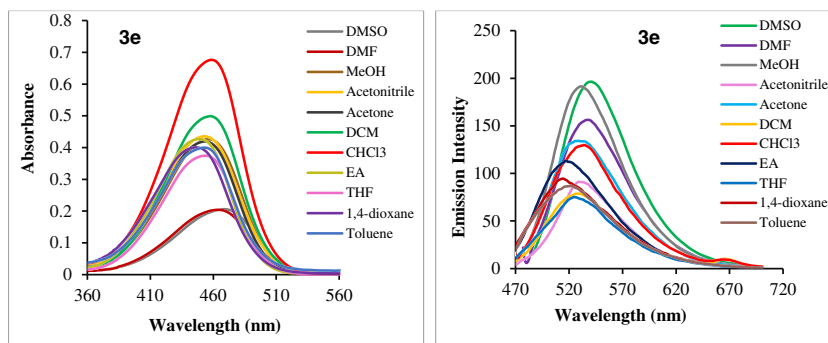


Dipole Moment Determination by Solvatochromic Method

The properties of solvents such as refractive index are dielectric constant are very important for study the physicochemical process of the dye molecules. These properties of solvent induce changes in the electronic transitions of solutes (solvatochromism) depending on the nature and the degree of interaction between the solute solvent in ground and first excited states of solutes (developed locally in the immediate vicinity) [48, 49]. The dipole moment of electronically excited species is of great importance in revelation of the nature of excited state, designing nonlinear optical material and parameterization of semi-empirical quantum chemical procedures of these states [50]. A most accepted technique for dipole moment calculation is based on Lippert-Mataga equation [51–54]. This technique is based on the absorption and emission maxima with polarity functions of solvents, expressed by the relative permittivity (ϵ) and refractive index (η) of the solvent medium [55, 56]. Hence solvatochromism and solvatofluorism are found to be excellent tools to evaluate the ground state and excited state dipole moments of the short-lived species [57–66].

The solvatochromic behaviour of the molecules was studied with the help of Lippert plot [51]. Lippert's plot is the plot of Stokes shift in cm^{-1} vs orientation polarizability. The Lippert function is constituted of the polarity function $f(\epsilon)$ and polarizability function $f(\eta)$ showed good correlation in less polar solvents which supports the charge transfer in the dyes **3a-3e** (Fig. S1).

Fig. 5 Absorption and emission spectra of compound **3e** in different solvent



Calculation of Dipole Moment

The solvent polarity functions $f_1(\epsilon, \eta)$ and $f_2(\epsilon, \eta)$ for each solvent were calculated by substituting the respective values for dielectric constant and refractive index in Eqs. (7) and (10) (SI) the values obtained are tabulated in Table S1. Graph of $f_1(\epsilon, \eta)$ versus Stokes shift in cm^{-1} is plotted and calculated m_1 as slope 1, as well as graph of $f_2(\epsilon, \eta)$ versus $(\bar{\nu}_a + \bar{\nu}_f)$ in cm^{-1} were plotted to get values of function m_2 as slope 2, the obtained values are tabulated in Table S1. Further ratio of excited state dipole moment to the ground state dipole moment is calculated from the Eq. 12 by substituting the values of m_1 and m_2 and summarized in Table S1. The compounds **3a** has higher μ_e/μ_g than **3b**, **3c**, **3d** and **3e** which suggest that the dyes with two electron withdrawing cyano group at acceptor part has more polar excited state. The dye **3d** has higher μ_e/μ_g ratio than **3c** because of effective charge transfer in the dye **3d** because of vacant d-orbitals of sulphur atom supports the charge transfer in the molecule. In the case of dye **3e**, higher μ_e/μ_g ratio was observed than **3b**, **3c**, **3d** because the extended conjugation present in the molecule facilitates charge transfer from donor to acceptor.

This observation is supported by DFT computations. We have calculated the dipole moment ratio computationally and detail values are given in the table (Table S2). The dipole moments of the molecules in the excited state were observed to be higher than in the ground state (Table S2).

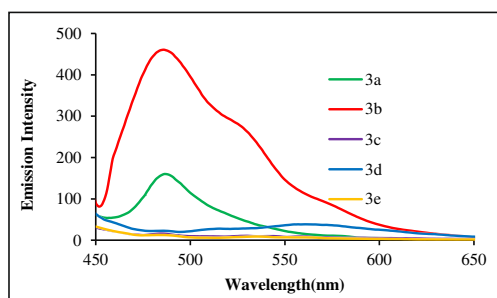


Fig. 6 Solid-state fluorescence spectra (normalized) of dyes **3a-3e** in powder form

Transition Dipole Moment

In addition to this the dipole moments between the excited and ground states the charge transfer character of the fluorophore can be understood from the oscillator strength (f) and transition dipole moment of the dyes (μ_a). The effective number of electrons transition from the ground to excited state is usually described by the oscillator strength, which provides the absorption area in the electronic spectrum. The oscillator strength (f) can be calculated using the following Eq. (2) [67–69].

$$f = 4.32 \times 10^{-9} \int \varepsilon(\nu) d\nu \quad (2)$$

Where,

ε is the extinction coefficient ($\text{L mol}^{-1} \text{cm}^{-1}$).

$\bar{\nu}$ represents the numerical value of wavenumber (cm^{-1}).

Transition dipole moments for absorption (μ_a) which is a measure of the probability of radiative transitions have been

calculated for the dyes different solvent environments using the Eq. (3) [70].

$$\mu_a^2 = \frac{f}{4.72 \times 10^{-7} \times \bar{\nu}} \quad (3)$$

The values of oscillator strength (f) and transition dipole moment (μ_a) for compound for each solvent is given in Table S3.

The observed higher values of transition dipole moments (μ_a) in less polar solvents indicates effective D- π -A charge transfer in the dyes **3a-3e** (Table S3).

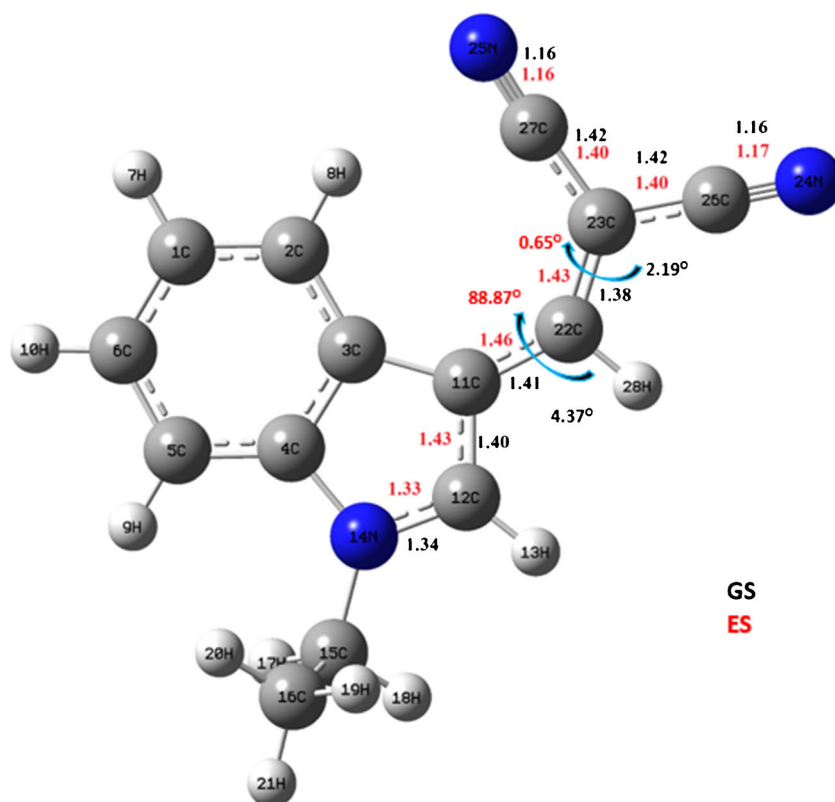
Optimized Geometries of Dyes 3a-3e

The ground state geometries of the dyes **3a** to **3e** were optimized at B3LYP/6-311 + G(d) level. In the case of dye **3a** the dihedral angle between indole moiety and acceptor part (C3-C11-C22-C23) in ground state is 4.37° whereas twisting was observed in excited state with dihedral angle 88.8° which suggest that the compound has almost planar geometry in ground state while nonplanar in excited state. This may be due to two strong electron withdrawing cyano groups present at the acceptor part (Fig. 7, Table S4, S5). The dihedral angle for **3a**, between double bond and electron withdrawing cyano group (C11-C22-C23-C27) in ground state is 2.2° and in excited state is 0.6° . This suggest that double bond C22-C23 and electron acceptor part constitutes planar geometry. The similar observation was observed for compound **3b** (Fig. S2, Table S4, S5). In the case of dye **3c** the dihedral angle between the indole unit

Table 2 Solid state emission photographs for dyes **3a-3e**

Dye	Day Light	UV Light	λ_{max} ems
3a			491 nm
3b			489 nm
3c			Not emissive
3d			570 nm
3e			Not emissive

Fig. 7 Optimized geometry parameters of dye **3a** in acetonitrile solvent in the ground state and excited state (bond length are in Å, dihedral angles are in degree)



and acceptor part in ground state was -6.4° and in excited state it was 0.8° , suggests the planar geometry of the compound (Fig. S3). The similar observation was observed for dye **3d** (Fig. S4, Table S4, S5). In the case of dye **3e** the dihedral angle between the indole core and the acceptor part (C3-C11-C22-C23) in GS and ES was 6.4 and 0.9° respectively which supports the planar geometry. The dihedral angle between the C22-C23-C25-C27 was in GS and ES, -157.4 and -179.9° respectively which supports the trans geometry of the double bond of **3e** (Fig. S5). In the excited state geometry, the major bond lengthening was observed between the bonds C12-C11, C11-C22, C22-C23, C25-C24 by 0.03, 0.05, 0.05 and 0.01 Å and bond length shorten for the bonds N14-C12, C23-C25, C23-C27 by 0.01, 0.02, 0.02 Å for the dye **3a** (Fig. 6). Similar observations are found for the dyes **3b-3e** (Table S4). Such lengthening and shortening of the bond lengths were due to the donor π acceptor charge transfer present in the molecules.

Electronic Vertical Excitation Spectra (TD-DFT)

The computed vertical excitation spectra associated with their oscillator strengths, composition, and assignments of the dyes as well as the corresponding experimental absorption wavelengths of the dyes **3a** to **3e** are shown in Table 3 and Table S6. The charge transfer band for donor π acceptor dyes are mainly due to the electronic transition from highest occupied molecular orbital (HOMO) to the lowest unoccupied molecular orbital (LUMO) Table 3 and Table S6 show that there is a

correlation between the experimentally obtained absorption wavelength maxima and TD-B3LYP/6-311 + G(d) computed vertical excitation of the synthesized dyes. The dye **3a** showed the blue shifted absorption in 1,4 dioxane (388 nm) and red shifted absorption in chloroform (400 nm). In the case compound **3a** the deviation between experimental absorption and vertical excitation in different solvents was ~ 30 nm. Similar observations were observed for compound **3b**, whereas less deviation is observed between experimental absorption and vertical excitation of the compounds **3c**, **3d** and **3e** in ethyl acetate, chloroform and 1,4 dioxane. In less polar solvent ethyl acetate, the compounds **3c**, **3d** show 4 nm deviation whereas **3e** shows 3 nm deviation in DMF, ACN, chloroform and toluene (Table S6). The experimentally obtained fluorescence emission spectral data and emission computed from TD-B3LYP/6-311 + G(d) computations are shown in Tables 3 and Table S6. All the dyes showed an increase in the emission wavelength increase in solvent polarity. A good correlation is seen between experimentally recorded emissions against the emissions computed from TD-B3LYP/6-311 + G(d) for the synthesized dyes in the different solvents.

Frontier Molecular Orbitals

The contribution of electronic transition from HOMO to LUMO is about 95 to 96 % in **3a** and 97 % for **3b**. The contribution of electronic transition from HOMO to LUMO is about 98 to 100 % in **3c**, **3d** and **3e**. Therefore, we confirm

Table 3 Observed UV-visible absorption and vertical excitation of compound **3a-3b** in different solvents

	Solvent	Experimental		TD-DFT						
		λ^a nm	λ^b nm	Vertical Exc ^c nm	ev	f^d	Assignment	% D ^e abs	TD-DFT Emission	% D ^f ems
3a	DMSO	398	443	360	3.4400	0.6949	H-L = 96 %	9.5	423	4.5
	DMF	398	442	361	3.4376	0.6979	H-L = 96 %	9.3	422	4.5
	ACN	394	444	359	3.4559	0.6751	H-L = 95 %	8.9	422	4.9
	MeOH	395	444	358	3.4595	0.6705	H-L = 95 %	9.4	423	4.7
	Acetone	398	443	359	3.4538	0.6778	H-L = 95 %	9.8	422	4.7
	DCM	397	436	360	3.4444	0.6912	H-L = 96 %	9.3	422	3.2
	CHCl ₃	400	436	360	3.4473	0.6913	H-L = 96 %	10.0	423	3.0
	EA	390	442	358	3.4589	0.6749	H-L = 96 %	8.2	423	4.3
	THF	391	440	359	3.4498	0.6851	H-L = 96 %	8.2	423	3.8
	1,4 dioxane	388	433	357	3.4697	0.6767	H-L = 96 %	8.0	428	1.2
	Toluene	398	443	359	3.4538	0.6946	H-L = 96 %	9.8	427	3.6
	DMSO	393	444	358	3.4624	0.7398	H-L = 97 %	8.9	409	7.9
	DMF	389	441	358	3.4604	0.7422	H-L = 97 %	8.0	409	7.2
	ACN	387	439	357	3.4778	0.7228	H-L = 97 %	7.8	409	6.8
	MeOH	391	443	356	3.4813	0.7189	H-L = 97 %	8.9	409	7.6
	3b	Acetone	387	433	357	3.4768	0.7248	H-L = 97 %	7.8	409
DCM		392	436	357	3.4701	0.7354	H-L = 97 %	9.3	409	6.2
CHCl ₃		393	437	357	3.4759	0.7343	H-L = 97 %	9.2	408	6.6
EA		386	434	356	3.4856	0.7209	H-L = 97 %	7.8	408	6.0
THF		384	432	357	3.4760	0.7299	H-L = 97 %	7.0	408	5.6
1,4 dioxane		384	433	354	3.5016	0.7200	H-L = 97 %	7.8	405	6.5
Toluene		387	437	356	3.4862	0.7354	H-L = 97 %	8.0	405	7.2

^a Experimental absorption wavelength^b Experimental emission wavelength^c Computed absorption wavelength^d Oscillator strength^e % Deviation between experimental absorption and vertical excitation computed by DFT^f % Deviation between experimental emission and computed (TD-DFT) emission

that the electronic transitions of dyes originate from HOMO to LUMO. As shown by molecular orbital diagrams (Table 4) of the dyes, the electron densities in the HOMO of all these dyes were largely located on donor indole unit and electron densities on the LUMO were found localised on the acceptor through carbon-carbon double bond. The HOMO levels of the dyes are mainly dominated by π -orbital contribution of the electron donor indole unit, while the LUMO levels are largely delocalized at the electron acceptor part (Table 4).

Linear Polarizability from DFT

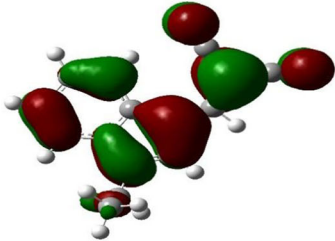
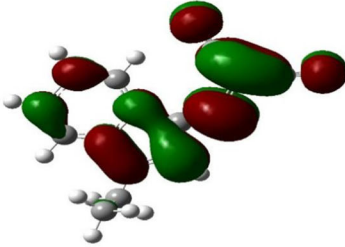
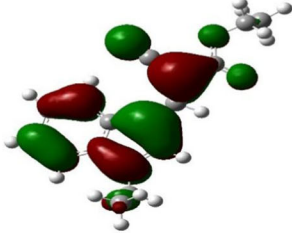
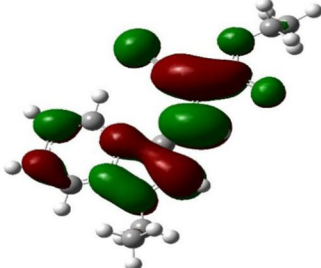
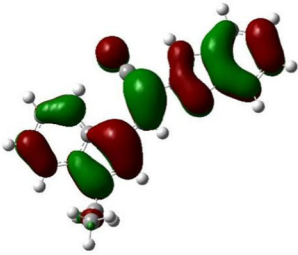
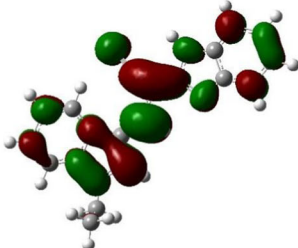
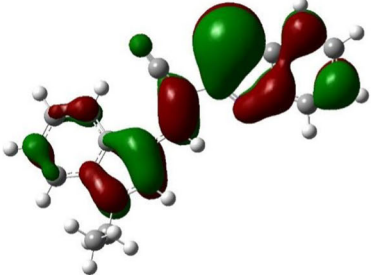
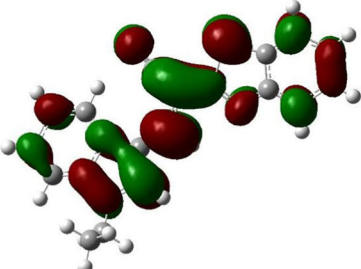
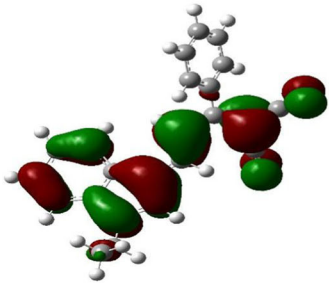
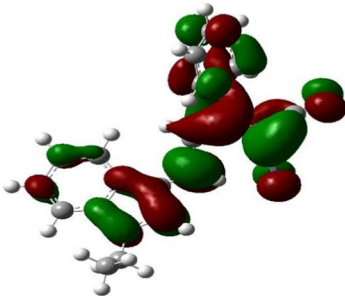
Theory to Calculate Nonlinear Optical (NLO) Properties by Theoretical Method

In this work we have also calculated dipole moment (μ), electronic polarizability (α), mean first hyperpolarizability (β_0) and second hyperpolarizability (γ) using B3LYP functional

with the 6-31G(d) basis set. For completeness, we will here briefly summarize the essential formulas used in our work, highlighting the quantities in which we are interested.

Here, second-order NLO properties of the carbazole based push pull chromophore **5a**, **5b**, **6a** and **6b** were calculated by using density functional theory (DFT). The static first hyperpolarizability (β_0) and second hyperpolarizability (γ) were calculated using B3LYP/6-31G(d) on the basis of the finite field approach [68, 71–73]. In the presence of an applied field, the energy of the system is a function of the electric field, and the first hyperpolarizability is a third rank tensor that can be described by a $3 \times 3 \times 3$ matrix. The 27 components of the 3D matrix can be reduced to 10 components because of the Kleinman symmetry [74]. The matrix can be given in the lower tetrahedral format. It is obvious that the lower part of the $3 \times 3 \times 3$ matrix is a tetrahedral. The components of β are defined as the co-efficient in the Taylor series expansion of the

Table 4 Frontier molecular orbital's of the compounds **3a** to **3e** in Acetonitrile

Dye	HOMO	LUMO
3a		
3b		
3c		
3d		
3e		

energy in the external electric field. When the external electric field is weak and homogeneous, this expansion becomes.

$$E = E^0 - \mu_a F_a - \frac{1}{2a_{\alpha\beta} F_a F_\beta} - \frac{1}{6\beta_{\alpha\beta\gamma} F_a F_\beta F_\gamma} + \dots \quad (4)$$

Where E^0 is the energy of the unperturbed molecules, F_a is the field at the origin, μ_a , $\alpha_{\alpha\beta}$ and $\beta_{\alpha\beta\gamma}$ are the components of dipole moment, polarizability and the first hyperpolarizabilities, respectively.

The total static dipole moment μ is expressed by following equation

$$\mu = \sqrt{\mu_x^2 + \mu_y^2 + \mu_z^2} \quad (5)$$

$$\beta_0 = \left[(\beta_{xxx} + \beta_{xyy} + \beta_{xzz})^2 + (\beta_{yxx} + \beta_{yyy} + \beta_{yzz})^2 + (\beta_{zxx} + \beta_{zyy} + \beta_{zzz})^2 \right]^{\frac{1}{2}} \quad (9)$$

Where, β_x , β_y , and β_z are the components of the second-order polarizability tensor along the x, y, and z axes.

The mean second hyperpolarizability (γ) is expressed by

$$\gamma = \frac{1}{5} \left[(\gamma_{xxxx} + \gamma_{yyyy} + \gamma_{zzzz}) + 2(\gamma_{xxyy} + \gamma_{yyzz} + \gamma_{zzxx}) \right] \quad (10)$$

Thus, these donor- π -acceptor chromophores have been studied due to their good linear and nonlinear optical properties. Second-order NLO properties of the donor- π -acceptor chromophores were calculated by using B3LYP/6-311 + G(d) on the basis of the finite field approach [75]. The computed mean polarizability (α_0), of the dyes **3a-e** were found to be ranging from 29.86×10^{-24} to 67.73×10^{-24} e.s.u (Table S7).

First Hyperpolarizability (β_0) by DFT

The donor - π - acceptor chromophores are expected to have good non-linear properties and their first hyperpolarizability (β_0) value can be enhanced due to their relative orientation. The computed first hyperpolarizability (β_0), of the dyes **3a-e** were found to be ranging from 12.64×10^{-30} to 168.41×10^{-30} e.s.u in the solvents (Table 5). These values are greater than urea 0.38×10^{-30} e.s.u. Thus these dyes show a large hyperpolarizability, suggesting considerable charge transfer characteristics from the donor to acceptor part. In polar solvents more hyperpolarability was observed then less polar solvents may be due to the effective π - π^* transition in polar solvents.

The isotropic polarizability can be calculated from the trace of the polarization tensor,

$$\alpha_0 = \frac{(a_{xx} + a_{yy} + a_{zz})}{3} \quad (6)$$

Anisotropy of the polarizability $\Delta\alpha$ is expressed by

$$\Delta\alpha = 2^{-1/2} \left[(a_{xx} + a_{yy})^2 + (a_{zz} + a_{xx})^2 + 6\alpha_{xx}^2 \right] \quad (7)$$

The mean first polarizability (β_0) is expressed by

$$\beta_0 = \left(\beta_x^2 + \beta_y^2 + \beta_z^2 \right)^{1/2} \quad (8)$$

Second Hyperpolarizability (γ) by DFT

The donor- π -acceptor styryls show very high γ values, both in DFT as well as the values obtained from solvatochromic method. The styryl shows γ values in the range of 33.62×10^{-36} to 450.35×10^{-36} esu. by DFT (Table S8).

Experimental Hyperpolarizability

The solvent dependent NLO properties of donor- π -acceptor styryls dyes were calculated [73, 76] The linear polarizability (α) value of extended styryls **3a-e** are tabulated in (Table S3). The first hyperpolarizability value of **3a - 3e** are found in the range of 5.68×10^{-30} to 23.0×10^{-30} e.s.u. These values are greater than urea (0.38×10^{-30} esu).

The third order hyperpolarizability $\langle \gamma \rangle_{SD}$ at molecular level originating from the electronic polarization in the non-

Table 5 Total first order hyperpolarizability (β_0) calculated with B3LYP/6-311 + G(d) for compound **3a-e**

Solvent	3a	3b	3c	3d	3e
DCM	–	41.19	25.88	77.88	168.41
CHCl ₃	–	36.86	20.59	66.64	144.31
EA	32.33	38.72	22.82	110.31	154.45
THF	33.74	40.14	24.56	74.33	162.42
1,4 dioxane	22.73	–	–	–	104.59
Toluene	23.57	–	12.64	50.57	–
Gas	12.83	18.60	22.23	29.77	58.92

Values in $\times 10^{-30}$ esu

resonant region can be treated by a three-level model and is expressed in literature [77–81]. The Quasi-two-level model in place of three level model using the density matrix formalism to a simpler Eq. (11) [82, 83].

$$\langle \gamma \rangle = \frac{1}{E_{eg}^3} \mu_{eg}^2 (\Delta\mu^2 - \Delta\mu_{eg}^2) \quad (11)$$

The third order hyperpolarizability that may be termed as the “solvatochromic descriptor” and the values calculated are tabulated in Table S9. The styryl dye **3e** shows more third order hyperpolarizability $\langle \gamma \rangle$ than other indole styryl dye may be due to extended conjugation present in the molecule.

Conclusion

In this paper we have designed and synthesized novel donor- π - acceptor styryl dyes containing indole as electron donor and -CN as an electron acceptor group. The photophysical properties are depends on solvent polarity. The absorption of the prepared dyes were in the region of 397–469 nm and emission in region of 432 nm to 554 nm. Due to the extended conjugation present in the dye **3e**, red shifted absorption and emission was observed as compare to dye **3a**, **3b**, **3c** and **3d**. The fluorescence spectra of indole styryl particularly **3a**, **3b** and **3d** in solid state was red shifted as compared to their fluorescence emission in less polar solvents. From the theoretical study it is observed that, the dyes showed more first hyperpolarability (β_0) in polar solvents than less polar solvents may be due to the effective π - π^* transition in polar solvents. The vertical excitation spectra were computed at B3LYP/6-311 + G(d) level and compared with the experimental values. The calculated results are in good accordance with the experimental values.

Acknowledgments Santosh Chemate (JRF/SRF) is thankful for fellowship from the Principal Scientific Adviser (PSA), Government of India.

References

- Matsui M, Ito A, Kotani M, et al. (2009) Dyes and pigments the use of indoline dyes in a zinc oxide dye-sensitized solar cell. *Dyes Pigments* 80:233–238. doi:10.1016/j.dyepig.2008.07.010
- Yu X, Ci Z, Liu T, et al. (2014) Influence of different electron acceptors in organic sensitizers on the performance of dye-sensitized solar cells. *Dyes Pigments* 102:126–132. doi:10.1016/j.dyepig.2013.10.045
- Pommeret S, Gustavsson T, Naskrecki R, et al. (1995) Femtosecond absorption and emission spectroscopy of the DCM laser dye. *J Mol Liq* 64:101–112. doi:10.1016/0167-7322(95)92824-U
- Shettigar S, Umesh G, Poornesh P, et al. (2009) Dyes and pigments the third-order nonlinear optical properties of novel styryl dyes. *Dyes Pigments* 83:207–210. doi:10.1016/j.dyepig.2009.04.009
- Huang JY, Lewis a, Loew L (1988) Nonlinear optical properties of potential sensitive styryl dyes. *Biophys J* 53:665–670. doi:10.1016/S0006-3495(88)83147-3
- Jha BN, Banerji JC (1985) Chromophoric chain β -aryl-substituted styryl cyanines: effect of substituents on visible absorption spectra and photosensitisation properties. *Dyes Pigments* 6:213–226. doi:10.1016/0143-7208(85)80018-8
- Hagberg DP, Yum JH, Lee H, et al. (2008) Novel near-infrared cyanine dyes for fluorescence imaging in biological systems. *J Am Chem Soc* 130:6259–6266. doi:10.1021/ja800066y
- Li Q, Lin G-L, Peng B-X, Li Z-X (1998) Synthesis, characterization and photographic properties of some new styryl cyanine dyes. *Dyes Pigments* 38:211–218. doi:10.1016/S0143-7208(97)00088-0
- Lee CC, Hu AT (2003) Synthesis and optical recording properties of some novel styryl dyes for DVD-R. *Dyes Pigments* 59:63–69. doi:10.1016/S0143-7208(03)00098-6
- Yashchuk VM, Yarmoluk SM, Kudrya VY, et al. (2008) Optical Biomedical Diagnostics: Sensors with Optical Response Based on Two-Photon Excited Luminescent Dyes for Biomolecules Detection. *Adv Opt Technol* 2008:1–11. doi:10.1155/2008/908246
- Park KH, Lee CJ, Song D, et al. (2001) Optical recording properties of styryl derivatives for digital versatile disc-recordable (DVD-R). *Mol Cryst Liq Cryst Sci Technol Sect A Mol Cryst Liq Cryst* 370:165–168. doi:10.1080/10587250108030062
- Sokołowska J, Podsiadły R, Stoczkiewicz J (2008) Styryl dyes as new photoinitiators for free radical polymerization. *Dyes Pigments* 77:510–514. doi:10.1016/j.dyepig.2006.11.011
- Haidekker M, Ling T, Anglo M, et al. (2001) New fluorescent probes for the measurement of cell membrane viscosity. *Chem Biol* 8:123–131. doi:10.1016/S1074-5521(00)90061-9
- Metsov S, Simov D, Stoyanov S, Nikolov P (1990) Photophysical characteristics of some 2-styrylindolium dyes. *Dyes Pigments* 13:11–19. doi:10.1016/0143-7208(90)80009-E
- Kim SD, Park EJ (2001) Relation between chemical structure of yellow disperse dyes and their lightfastness. *Fibers Polym* 2:159–163. doi:10.1007/BF02875330
- Chung S-J, Zheng S, Odani T, et al. (2006) Extended squaraine dyes with large two-photon absorption cross-sections. *J Am Chem Soc* 128:14444–14445. doi:10.1021/ja065556m
- Lee H-S, Kim S-K, Lee W-J, et al. (2001) Synthesis and properties of organic light-emitting diodes using new emissive materials. *Mol Cryst Liq Cryst Sci Technol Sect A Mol Cryst Liq Cryst* 370:39–42. doi:10.1080/10587250108030034
- Fei X, Gu Y, Li C, et al. (2013) Synthesis and spectra of a kind of novel longer-wavelength benzoxazole indole styryl cyanine dye with a carbazole-bridged chain. *J Fluoresc* 23:221–226. doi:10.1007/s10895-012-1137-y
- Babür B, Seferoğlu N, Aktan E, et al. (2014) Phenylazindole dyes 2: the molecular structure characterizations of new phenylazo indoles derived from 1,2-dimethylindole. *Dyes Pigments* 103:62–70. doi:10.1016/j.dyepig.2013.11.019
- Greaves A, Daubresse N (2009) Thiol/disulfide indole-derived, styryl dye, dye composition comprising said dye, for lightening keratin materials using this dye. WO2009037325 A2
- Application F, Data P (2010) (12) United States Patent. 2:
- Mitschke U, Bäuerle P (2000) The electroluminescence of organic materials. *J Mater Chem* 10:1471–1507. doi:10.1039/a908713c
- Chen C-T (2004) Evolution of red organic light-emitting diodes: materials and devices. *Chem Mater* 16:4389–4400. doi:10.1021/cm049679m
- D’Andrade BW, Forrest SR (2004) White organic light-emitting devices for solid-state lighting. *Adv Mater* 16:1585–1595. doi:10.1002/adma.200400684
- Song Y, Di C, Yang X, et al. (2006) A cyclic triphenylamine dimer for organic field-effect transistors with high performance. *J Am Chem Soc* 128:15940–15941. doi:10.1021/ja064726s

26. De S, Das S, Girigoswami A (2005) Environmental effects on the aggregation of some xanthenes dyes used in lasers. *Spectrochim Acta A Mol Biomol Spectrosc* 61:1821–1833. doi:10.1016/j.saa.2004.06.054
27. Liao L, Dai L, Smith A, et al. (2007) Photovoltaic-active Dithienosilole-containing polymers. *Macromolecules* 40:9406–9412. doi:10.1021/ma071825x
28. Asefa A, Singh AK (2009) A fluorescence study of novel styrylindoles in homogenous and microheterogeneous media. *J Fluoresc* 19:921–930. doi:10.1007/s10895-009-0525-4
29. Asefa A, Singh AK (2010) Fluorescence emission enhancement in substituted 3-styrylindoles in the solid state. *J Lumin* 130:24–28. doi:10.1016/j.jlumin.2009.07.016
30. McDonagh C, Burke CS, MacCraith BD (2008) Optical chemical sensors. *Chem Rev* 108:400–422. doi:10.1021/cr068102g
31. Li Q, Lee JS, Ha C, et al. (2004) Solid-phase synthesis of styryl dyes and their application as amyloid sensors. *Angew Chem Int Ed* 43:6331–6335. doi:10.1002/anie.200461600
32. Hong Y, Lam JWY, Tang BZ (2011) Aggregation-induced emission. *Chem Soc Rev* 40:5361. doi:10.1039/c1cs15113d
33. Wu Q, Peng Q, Niu Y, et al. (2012) Theoretical insights into the aggregation-induced emission by hydrogen bonding: a QM/MM study. *J Phys Chem A* 116:3881–3888. doi:10.1021/jp3002367
34. Wang B, Qian Y (2013) Synthesis and efficient solid-state emission of conjugated donor–acceptor–donor triphenylamine chromophores. *New J Chem* 37:1402. doi:10.1039/c3nj41115j
35. Rao KV, Datta KKR, Eswaramoorthy M, George SJ (2013) Highly pure solid-state white-light emission from solution-processable soft-hybrids. *Adv Mater* 25:1713–1718. doi:10.1002/adma.201204407
36. Matsui M, Ooiwa K, Okada A, et al. (2013) Dyes and pigments solid-state fluorescence of pyridinium styryl dyes. *Dyes Pigments* 99:916–923. doi:10.1016/j.dyepig.2013.07.026
37. Gupta VD, Tathe AB, Padalkar VS, et al. (2013) Red emitting solid state fluorescent triphenylamine dyes: synthesis, photo-physical property and DFT study. *Dyes Pigments* 97:429–439. doi:10.1016/j.dyepig.2012.12.024
38. Wang Q, Liu H, Lu H, et al. (2013) Synthesis, characterization and solid-state emission properties of arylsilyl-substituted pyrene derivatives. *Dyes Pigments* 99:771–778. doi:10.1016/j.dyepig.2013.07.003
39. Frisch MJ, Trucks GW, Schlegel HB, et al. (2009) Gaussian 09, Revision C.01. Gaussian 09, Revis. B.01, Gaussian, Inc., Wallingford CT
40. Cancès E, Mennucci B, Tomasi J (1997) A new integral equation formalism for the polarizable continuum model: theoretical background and applications to isotropic and anisotropic dielectrics. *J Chem Phys* 107:3032. doi:10.1063/1.474659
41. Treutler O, Ahlrichs R (1995) Efficient molecular numerical integration schemes. *J Chem Phys* 102:346. doi:10.1063/1.469408
42. Becke AD (1993) A new mixing of Hartree–Fock and local density-functional theories. *J Chem Phys* 98:1372. doi:10.1063/1.464304
43. Lee C, Yang W, Parr RG (1988) Development of the Colle–Salvetti correlation-energy formula into a functional of the electron density. *Phys Rev B* 37:785–789. doi:10.1103/PhysRevB.37.785
44. Meech SR, Phillips D (1983) Photophysics of some common fluorescence standards. *J Photochem* 23:193–217. doi:10.1016/0047-2670(83)80061-6
45. Saroj MK, Sharma N, Rastogi RC (2011) Solvent effect profiles of absorbance and fluorescence spectra of some indole based chalcones. *J Fluoresc* 21:2213–2227. doi:10.1007/s10895-011-0926-z
46. Xu H, Fan L-L (2011) Antifungal agents. Part 4: synthesis and antifungal activities of novel indole[1,2-c]-1,2,4-benzotriazine derivatives against phytopathogenic fungi in vitro. *Eur J Med Chem* 46:364–369. doi:10.1016/j.ejmech.2010.10.022
47. Rajagopal B, Chou CH, Chung CC, Lin PC (2014) Synthesis of substituted 3-indolylimines and indole-3-carboxaldehydes by rhodium(II)-catalyzed annulation. *Org Lett* 16:3752–3755. doi:10.1021/ol501618z
48. Ghanadzadeh Gilani A, Moghadam M, Zakerhamidi MS (2012) Solvatochromism of Nile red in anisotropic media. *Dyes Pigments* 92:1052–1057. doi:10.1016/j.dyepig.2011.07.018
49. Hermant RM, Bakker NAC, Scherer T, et al. (1990) Systematic study of a series of highly fluorescent rod-shaped donor–acceptor systems. *J Am Chem Soc* 112:1214–1221. doi:10.1021/ja00159a050
50. Ravi M, Samanta A, Radhakrishnan TP (1994) Excited state dipole moments from an efficient analysis of Solvatochromic Stokes shift data. *J Phys Chem* 98:9133–9136. doi:10.1021/j100088a007
51. Lippert E (1957) Spektroskopische Bestimmung des Dipolmomentes aromatischer Verbindungen im ersten angeregten Singulettzustand. *Zeitschrift für Elektrochemie, Berichte der Bunsengesellschaft für Phys Chemie* 61:962–975. doi:10.1002/bbpc.19570610819
52. Mataga N (1963) Solvent effects on the absorption and fluorescence spectra of Naphthylamines and isomeric Aminobenzoic acids. *Bull Chem Soc Jpn* 36:654–662. doi:10.1246/bcsj.36.654
53. Mataga N, Kaifu Y, Koizumi M (1955) The solvent effect on fluorescence spectrum, change of solute–solvent interaction during the lifetime of excited solute molecule. *Bull Chem Soc Jpn* 28:690–691. doi:10.1246/bcsj.28.690
54. Mataga N, Kaifu Y, Koizumi M (1956) Solvent effects upon fluorescence spectra and the dipolemoments of excited molecules. *Bull Chem Soc Jpn* 29:465–470. doi:10.1246/bcsj.29.465
55. Christian Reichardt *Solvents and Solvent Effects in Organic Chemistry*. Third, Upd: Wiley VCH Verlag GmbH & Co. KGaA, Weinheim.
56. Reichardt C (1994) Solvatochromic dyes as solvent polarity indicators. *Chem Rev* 94:2319–2358. doi:10.1021/cr00032a005
57. Ravi M, Soujanya T, Samanta A, Radhakrishnan TP (1995) Excited-state dipole moments of some Coumarin dyes from a solvatochromic method using the solvent polarity parameter, E N T. *J Chem Soc Faraday Trans* 91:2739. doi:10.1039/ft9959102739
58. Kumar S, Rao V, Rastogi R (2001) Excited-state dipole moments of some hydroxycoumarin dyes using an efficient solvatochromic method based on the solvent polarity parameter, ETN. *Spectrochim Acta Part A Mol Biomol Spectrosc* 57:41–47. doi:10.1016/S1386-1425(00)00330-9
59. Masternak A, Wenska G, Milecki J, et al. (2005) Solvatochromism of a novel betaine dye derived from purine. *J Phys Chem A* 109:759–766. doi:10.1021/jp047098e
60. Nemkovich NA, Pivovarenko VG, Baumann W, et al. (2005) Dipole moments of 4'-aminoflavonol fluorescent probes in different solvents. *J Fluoresc* 15:29–36. doi:10.1007/s10895-005-0210-1
61. Aaron JJ, Maafi M, Kersebet C, et al. (1996) A solvatochromic study of new benzo[a]phenothiazines for the determination of dipole moments and specific solute–solvent interactions in the first excited singlet state. *J Photochem Photobiol A Chem* 101:127–136. doi:10.1016/S1010-6030(96)04442-5
62. Harbison GS (2002) The electric dipole polarity of the ground and low-lying metastable excited states of NF. *J Am Chem Soc* 124:366–367. doi:10.1021/ja0159261
63. Raikar US, Renuka CG, Nadaf YF, et al. (2006) Rotational diffusion and solvatochromic correlation of coumarin 6 laser dye. *J Fluoresc* 16:847–854. doi:10.1007/s10895-006-0126-4
64. Nadaf YF, Mulimani BG, Gopal M, Inamdar SR (2004) Ground and excited state dipole moments of some exalite UV laser dyes from solvatochromic method using solvent polarity parameters. *J Mol Struct THEOCHEM* 678:177–181. doi:10.1016/j.theochem.2004.01.049
65. Józefowicz M, Heldt JR (2007) Dipole moments studies of fluorenone and 4-hydroxyfluorenone. *Spectrochim Acta Part A Mol Biomol Spectrosc* 67:316–320. doi:10.1016/j.saa.2006.07.019

66. Biradar DS, Siddlingeshwar B, Hanagodimath SM (2008) Estimation of ground and excited state dipole moments of some laser dyes. *J Mol Struct* 875:108–112. doi:10.1016/j.molstruc.2007.04.005
67. Turro NJ (1978) *Modern Molecular Photochemistry*. Benjamin-Cummings, New York
68. Lanke SK, Sekar N (2015) Rigid Coumarins: a Complete DFT, TD-DFT and Non Linear Optical Property Study. *J Fluoresc*. doi:10.1007/s10895-015-1638-6
69. Telore RD, Satam M a, Sekar N (2015) NLOphoric studies in thiazole containing symmetrical push – pull fluorophores – Combined experimental and DFT approach. *Opt Mater (Amst)* 48:271–280. doi:10.1016/j.optmat.2015.08.006
70. Coe BJ, Harris JA, Asselberghs I, et al. (2002) Quadratic nonlinear optical properties of N-aryl Stilbazolium dyes. *Adv Funct Mater* 12: 110–116. doi:10.1002/1616-3028(20020201)12:2<110::AID-ADFM110>3.0.CO;2-Y
71. Ditchfield R, Hehre WJ, Pople JA (1971) Self-consistent molecular-orbital methods. IX An extended Gaussian-type basis for molecular-orbital studies of organic molecules. *J Chem Phys* 54: 724–728. doi:10.1063/1.1674902
72. Hehre WJ, Ditchfield R, Pople JA (1972) Self-consistent molecular orbital methods. XII. Further extensions of Gaussian-type basis sets for use in molecular orbital studies of organic molecules. *J Chem Phys* 56:2257–2261. doi:10.1063/1.1677527
73. Lanke SK, Sekar N (2016) Aggregation induced emissive carbazole-based push pull NLOphores: synthesis, photophysical properties and DFT studies. *Dyes Pigments* 124:82–92. doi:10.1016/j.dyepig.2015.09.013
74. Kleinman DA (1962) Nonlinear dielectric polarization in optical media. *Phys Rev* 126:1977–1979. doi:10.1103/PhysRev.126.1977
75. Vidya S, Ravikumar C, Hubert Joe I, et al. (2011) Vibrational spectra and structural studies of nonlinear optical crystal ammonium D, L-tartrate: a density functional theoretical approach. *J Raman Spectrosc* 42:676–684. doi:10.1002/jrs.2743
76. Telore RD, Satam M a, Sekar N (2015) Push–pull fluorophores with viscosity dependent and aggregation induced emissions insensitive to polarity. *Dyes Pigments* 122:359–367. doi:10.1016/j.dyepig.2015.07.017
77. Oudar JL (1977) Optical nonlinearities of conjugated molecules. Stilbene derivatives and highly polar aromatic compounds. *J Chem Phys* 67:446. doi:10.1063/1.434888
78. De PR (1982) Nonlinear-Optical Properties. *Phys Rev A* 26:2016–1027
79. Kwon OP, Jazbinsek M, Seo JI, et al. (2010) First hyperpolarizability orientation in asymmetric pyrrole-based polyene chromophores. *Dyes Pigments* 85:162–170. doi:10.1016/j.dyepig.2009.10.019
80. Weaver CS, Smith SW, Hyndman RD, et al. (1991) 0.028. *Science* 252:103–106
81. Cheng L-T, Tam W, Stevenson SH, et al. (1991) Experimental investigations of organic molecular nonlinear optical polarizabilities. 1. Methods and results on benzene and stilbene derivatives. *J Phys Chem* 95:10631–10643. doi:10.1021/j100179a026
82. Dirk CW, Cheng L-T, Kuzyk MG (1992) A simplified three-level model describing the molecular third-order nonlinear optical susceptibility. *Int J Quantum Chem* 43:27–36. doi:10.1002/qua.560430106
83. Kuzyk MG, Dirk CW (1990) Effects of centrosymmetry on the nonresonant electronic third-order nonlinear optical susceptibility. *Phys Rev A* 41:5098–5109. doi:10.1103/PhysRevA.41.5098